CMS TN/94-138
27 January 1994

Estimation of the RPC Muon Trigger Rates Due to Neutral Particles

M. Huhtinen
Research Institute for High Energy Physics, University of Helsinki, Finland

G. Wrochna
CERN, Geneva, Switzerland
on leave of absence from Institute of Experimental Physics, Warsaw University, Poland

A high level of neutral particle background is expected in LHC detectors. The aim of the study presented in this note is to estimate how this background effects the first level muon trigger.

1 Hit rates

Fluxes of low momentum neutrons and photons in the CMS detector have been calculated for various shielding setups [1, 2]. In order to estimate rates of hits in Resistive Plate Chambers (RPC) let us assume that the efficiency of RPC for neutrons is 0.0005, for photons is 0.005, and for charged particles is 1, independently of the incoming rate. Resulting rates for RPCs placed in the forward muon stations are given in Tab. 1. Since the rates in the barrel are significantly lower than those in the forward part of the detector, we have concentrated here on the region $1.5 < |\eta| < 2.5$.

Table 1: Hit rates [Hz/cm^2] in RPC due to neutron's and γ's.

shielding setup 4											
		η_{min}									
		1.5	1.6	1.7	1.8	1.9	2.0	2.1	2.2	2.3	2.4
MF1	n	3	5	6	11	19	31	45	53	56	57
	γ	64	97	118	213	381	522	636	881	1255	1443
MF2	n	1	2	5	9	14	21	31	40	51	56
	γ	36	67	121	178	238	315	409	606	907	1057
MF3	n	2	4	7	11	17	28	44	62	83	93
	γ	36	51	77	114	164	304	534	836	1210	1397
MF4	n	24	27	32	37	42	55	76	97	116	126
	γ	885	1019	1134	1076	847	891	1207	1992	3246	3873

shielding setup 6											
		η_{min}									
		1.5	1.6	1.7	1.8	1.9	2.0	2.1	2.2	2.3	2.4
MF1	n	8	14	21	36	57	87	125	164	203	223
	γ	72	125	181	269	387	532	705	923	1187	1320
MF2	n	4	9	17	28	43	64	93	134	187	213
	γ	37	61	94	152	235	341	469	605	751	824
MF3	n	4	8	13	24	40	65	100	144	199	226
	γ	31	45	65	108	174	260	365	466	560	608
MF4	n	31	32	34	38	45	65	97	142	201	231
	γ	414	415	359	345	373	501	730	998	1304	1457

shielding setup 7											
		η_{min}									
		1.5	1.6	1.7	1.8	1.9	2.0	2.1	2.2	2.3	2.4
MF1	n	7	11	14	20	29	43	63	76	82	86
	γ	154	275	413	566	736	1053	1518	2178	3033	3461
MF2	n	3	5	9	17	28	43	63	82	100	109
	γ	71	119	194	283	384	553	788	1229	1877	2201
MF3	n	4	6	10	16	25	37	52	69	87	97
	γ	49	79	114	172	253	433	715	1080	1529	1753
MF4	n	32	37	39	45	55	70	91	113	136	147
	γ	270	350	427	513	606	896	1383	2018	2801	3192

shielding setup 8											
		η_{min}									
		1.5	1.6	1.7	1.8	1.9	2.0	2.1	2.2	2.3	2.4
MF1	n	4	9	16	26	37	51	69	80	85	87
	γ	123	217	321	475	677	1034	1546	2214	3039	3452
MF2	n	2	4	7	13	22	36	53	72	93	104
	γ	66	111	176	275	410	649	992	1517	2225	2579
MF3	n	4	6	9	16	27	42	62	82	101	111
	γ	79	105	144	260	453	672	917	1392	2099	2453
MF4	n	13	14	15	20	28	45	69	87	99	105
	γ	876	872	720	645	648	873	1319	1955	2779	3192

2 Trigger configuration

We have studied the trigger configuration as described in [2, 3, 4]. In the discussed region the trigger is based on four RPC planes (one per station). Each plane consists of strips having a size of $\Delta\varphi = 1/3^0 \;\times\; \Delta\eta = 0.1$. Physical size of the strips is given in Tab. 2.

Table 2: RPC strip sizes [cm].

		η_{min}									
		1.5	1.6	1.7	1.8	1.9	2.0	2.1	2.2	2.3	2.4
MF1	length	30.2	26.6	23.6	21.0	18.8	16.8	15.1	13.5	12.2	10.9
	width	1.6	1.4	1.3	1.2	1.0	0.9	0.9	0.8	0.7	0.6
MF2	length	38.2	33.7	29.9	26.6	23.8	21.3	19.1	17.1	15.4	13.9
	width	2.0	1.8	1.6	1.5	1.3	1.2	1.1	1.0	0.9	0.8
MF3	length	43.3	38.2	33.9	30.2	26.9	24.1	21.6	19.4	17.5	15.7
	width	2.3	2.1	1.9	1.7	1.5	1.4	1.2	1.1	1.0	0.9
MF4	length	47.7	42.1	37.3	33.2	29.7	26.5	23.8	21.4	19.2	17.3
	width	2.5	2.3	2.0	1.8	1.7	1.5	1.3	1.2	1.1	1.0

A muon traversing the detector hits the RPC strips on its way. The observed four hit pattern is compared with a predefined set of valid patterns. The positive trigger decision is taken if the observed pattern is found among the valid patterns for a given p_t^{cut}. Table 3 gives the number of valid patterns for several p_t^{cut} values in various $|\eta|$ intervals.

Table 3: Number of valid patterns.

p_t^{cut}		η_{min}									
index	GeV/c	1.5	1.6	1.7	1.8	1.9	2.0	2.1	2.2	2.3	2.4
1	1.0	2575	3514	3480	3447	3166	3401	3810	3790	4352	3354
2	1.5	2575	3514	3480	3447	3166	3401	3810	3790	4352	3354
3	2.0	2575	3514	3480	3447	3166	3401	3810	3714	3334	2524
4	2.5	2575	3514	3480	3447	3158	2929	2585	2387	2050	1625
5	3.0	2559	3514	3291	3069	2318	2016	1782	1529	1287	1025
6	3.5	2277	2946	2556	2166	1653	1386	1168	988	776	635
7	4.0	1507	2114	1828	1543	1125	947	748	656	497	437
8	4.5	1025	1544	1319	1094	747	616	532	452	376	331
9	5.0	750	1115	932	749	542	436	389	324	271	239
10	5.5	582	790	660	530	383	332	302	258	211	190
11	6.0	438	580	490	400	306	264	217	202	171	152
12	7.0	265	338	295	252	193	171	154	134	122	111
13	10.0	111	135	123	112	91	84	73	70	62	56
14	15.0	53	62	57	52	48	43	41	37	35	33
15	20.0	35	43	39	35	30	31	27	23	22	23
16	30.0	22	25	22	19	17	17	16	15	14	13
17	50.0	13	13	13	13	11	11	11	9	9	7
18	70.0	11	11	10	10	8	7	7	7	7	7
19	100.0	7	7	7	7	7	7	7	7	7	7
20	150.0	6	6	6	6	6	6	6	6	6	6

3 Basic formulae

Let us consider a sector $\Delta\varphi = 30^0 \quad \times \quad \Delta\eta \approx 0.1$ (one strip length).

Let us denote:

$r_m^{n,\gamma}(\eta)$ [Hz/cm^2]	– noise rate at station m
$s_m(\eta)$ [cm^2]	– strip area (for MF1-3 s_m should contain η-neighbouring strips)
$N_{s/s} = 90$	– number of strips per sector
$N_{all} = N_{s/s}^4$	– number of all possible patterns of strips in 4 stations
$N_{val}(p_t^{cut}, \eta)$	– number of valid patterns
$t_{bunch} = 25$ ns	– bunch crossing interval
$t_{gate} = 25$ ns	– trigger coincidence gate

The reason for including the area of neighbouring strips is that they will be OR-ed together to pick-up muons crossing the border of two segments.

In the formulae the parameter η is omited since the index "*sect*" already indicates that the denoted variables can have different values for different sectors.

Probability that a single strip is hit:

$$P_m^{hit} = t_{gate} r_m^{n,\gamma} s_m \tag{1}$$

Probability of any 4-fold coincidence:

$$P_{sect}^{coinc} = \prod_{m=1}^{4} N_{s/s} P_m^{hit} \tag{2}$$

Trigger probability:

$$P_{sect}^{trig}(p_t^{cut}) = \frac{N_{s/s} N_{val}(p_t^{cut})}{N_{all}} P_{sect}^{coinc} = \frac{N_{s/s} N_{val}(p_t^{cut})}{N_{s/s}^4} P_{sect}^{coinc} = N_{s/s} N_{val}(p_t^{cut}) \prod_{m=1}^{4} P_m^{hit} \tag{3}$$

Trigger rate in a sector [Hz]:

$$\begin{gathered} R_{sect}^{n,\gamma}(p_t^{cut}) = P_{sect}^{trig}(p_t^{cut})/t_{bunch} = \\ = N_{s/s} N_{val}(p_t^{cut}) \textstyle\prod_{m=1}^{4} P_m^{hit}/t_{bunch} = N_{s/s} N_{val}(p_t^{cut}) \frac{t_{gate}^4}{t_{bunch}} \prod_{m=1}^{4} r_m^{n,\gamma} s_m \end{gathered} \tag{4}$$

Total trigger rate [Hz]:

$$R^{n,\gamma}(p_t^{cut}) = \sum_{sect} R_{sect}^{n,\gamma}(p_t^{cut}) \tag{5}$$

The trigger rates calculated for the input values given above are plotted in Fig. 1 as a function of rapidity and momentum.

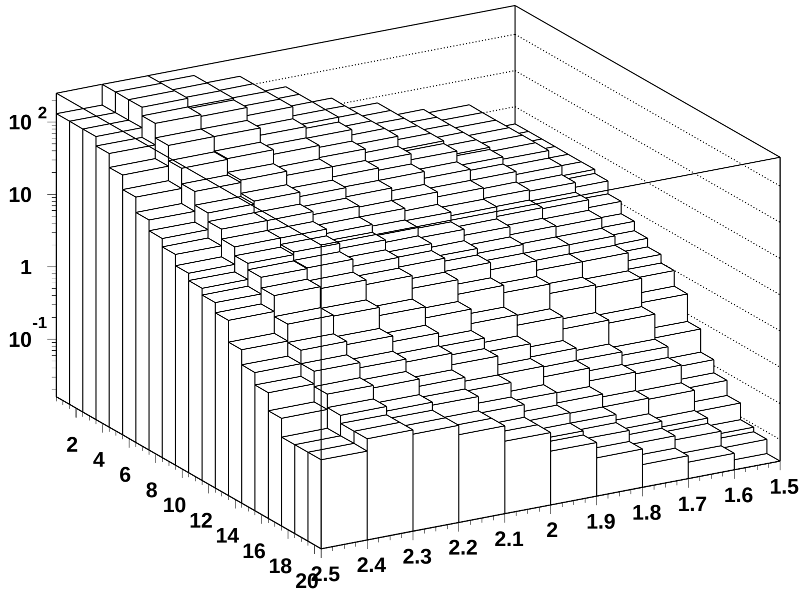

Figure 1: Rate [Hz/$\Delta\eta$] vs p_t^{cut} bin (see Tab. 3) and η.

4 Accounting for dead areas

Deriving the above formulas we assumed that acceptance of the detector is 100 %. However a real detector always has some unavoidable dead areas. In order to account for geometrical inefficiencies one can trigger if any 3 out of 4 stations are hit, i.e. only 3-fold coincidence is required. This is equivalent to the assumption that all strips in the missing station are hit. However, to avoid too many ghosts one can request that only dead areas of the missing station are hit and there is at most one such an artificial hit in the pattern (see Fig. 2). This means that 3-fold coincidence is accepted only in dead regions.

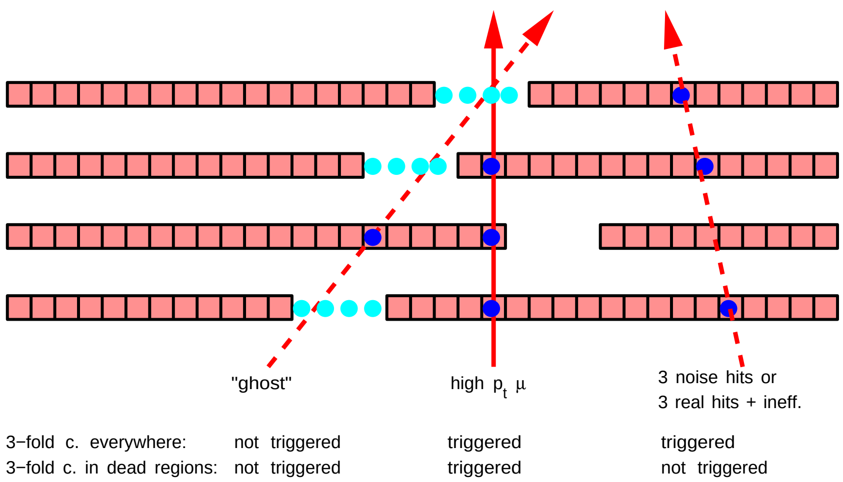

Figure 2: Difference between the two ways of treating geometrical inefficiencies (see text).

If we denote a dead fraction of station m by P_m^{dead}($\approx 10\%$) then a given pattern appears in the first cases (3-fold coincidence everywhere) with the probability

$$P'_{3/4} = (1-P_1^{dead})P_1^{hit}\cdot(1-P_2^{dead})P_2^{hit}\cdot(1-P_3^{dead})P_3^{hit}\cdot(P_4^{dead}P_4^{hit} + 1-P_4^{hit}) \ + \ perm. \quad (6)$$

Since P_m^{hit} does not exceed 0.003

$$P'_{3/4} \approx (1-P_1^{dead})P_1^{hit}\cdot(1-P_2^{dead})P_2^{hit}\cdot(1-P_3^{dead})P_3^{hit} \ + \ perm. \quad (7)$$

In the second case (3-fold coincidence only in dead regions)

$$P''_{3/4} = (1-P_1^{dead})P_1^{hit}\cdot(1-P_2^{dead})P_2^{hit}\cdot(1-P_3^{dead})P_3^{hit}\cdot P_4^{dead} \ + \ perm. \quad (8)$$

Note that if all P_m^{dead} are equal, the two formulae differ by factor P^{dead}. Probability of any 3-fold coincidence is now given by:

$$P_{sect,3/4}^{coinc} = N_{s/s}^3 P_{3/4} \quad \text{where} \quad P_{3/4} = P'_{3/4} \text{ or } P''_{3/4} \quad (9)$$

Following formulas modify accordingly. Trigger probability:

$$P_{sect,3/4}^{trig}(p_t^{cut}) = \frac{N_{s/s}N_{val}(p_t^{cut})}{N_{all}}P_{sect,3/4}^{coinc} = \frac{N_{s/s}N_{val}(p_t^{cut})}{N_{s/s}^4}P_{sect,3/4}^{coinc} = N_{val}(p_t^{cut})P_{3/4} \quad (10)$$

Trigger rate in a sector [Hz]:

$$R_{sect,3/4}^{n,\gamma}(p_t^{cut}) = P_{sect}^{trig}(p_t^{cut})/t_{bunch} = N_{val}(p_t^{cut})P_{3/4}/t_{bunch} \quad (11)$$

Total trigger rate [Hz]:

$$R_{3/4}^{n,\gamma}(p_t^{cut}) = \sum_{sect} R_{sect,3/4}^{n,\gamma}(p_t^{cut}) \quad (12)$$

Probability of any 4-fold coincidence is now also modified:

$$P_{sect,4/4}^{coinc} = \prod_{m=1}^{4} N_{s/s}P_m^{hit}(1-P_m^{dead}) \quad (13)$$

which leads to modified formulas on the trigger rate in a sector:

$$R_{sect,4/4}^{n,\gamma}(p_t^{cut}) = N_{s/s}N_{val}(p_t^{cut})\frac{t_{gate}^4}{t_{bunch}}\prod_{m=1}^{4} r_m^{n,\gamma}s_m(1-P_m^{dead}) \quad (14)$$

$$R_{4/4}^{n,\gamma}(p_t^{cut}) = \sum_{sect} R_{sect,4/4}^{n,\gamma}(p_t^{cut}) \quad (15)$$

Finally:

$$R_{total}^{n,\gamma} = R_{3/4}^{n,\gamma} + R_{4/4}^{n,\gamma} \quad (16)$$

5 Results

Results obtained assuming shielding setup 6 [1] (actually the best one) and $P^{dead} = 10\%$ are presented in Figs 3 and 4. The rate of real muons is also indicated (dashed curves). The two methods of taking a 3-fold coincidence are compared in Fig 3. As we already mentioned, restricting of the 3-fold coincidence to dead areas reduces the rate by factor $1/P^{dead}$ (10 times in this case) and therefore is strongly preferable. Hereafter we consider only this solution.

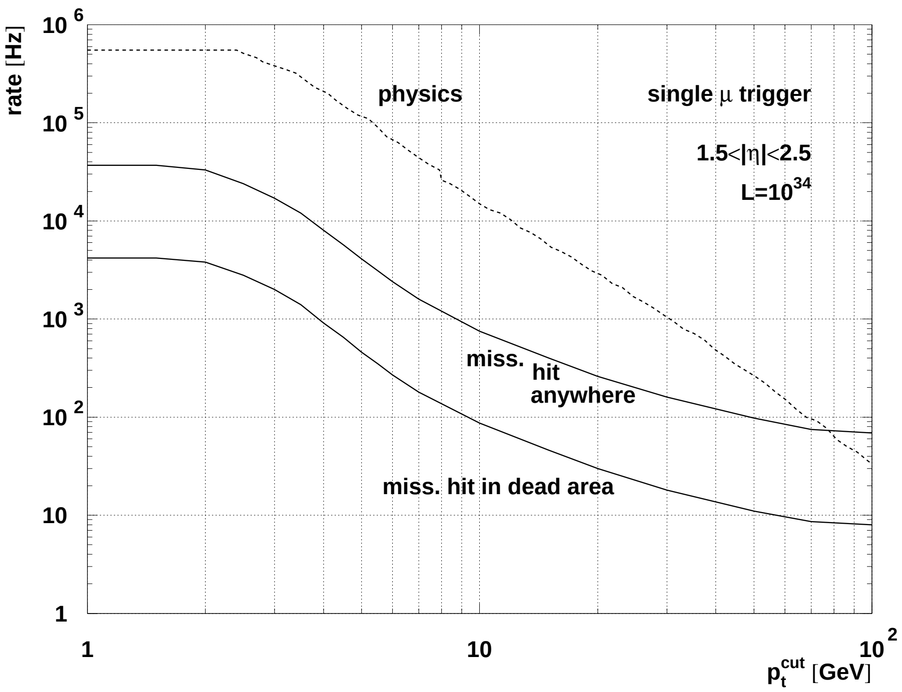

Figure 3: Trigger rate due to n's and γ's for any 3-fold coincidence and with 4th hit in a dead area.

The rates coming from 3-fold and 4-fold coincidences are compared in Fig 4. It is seen that $R^{n,\gamma}_{4/4}$ is negligible in compare to $R^{n,\gamma}_{3/4}$. In fact $R^{n,\gamma}_{3/4}$ dominates already if $P^{dead} > 10\%$.

The Fig. 5 shows how the total rate depends on the fraction of dead area. The dependence is significant which gives one more argument for minimizing dead areas.

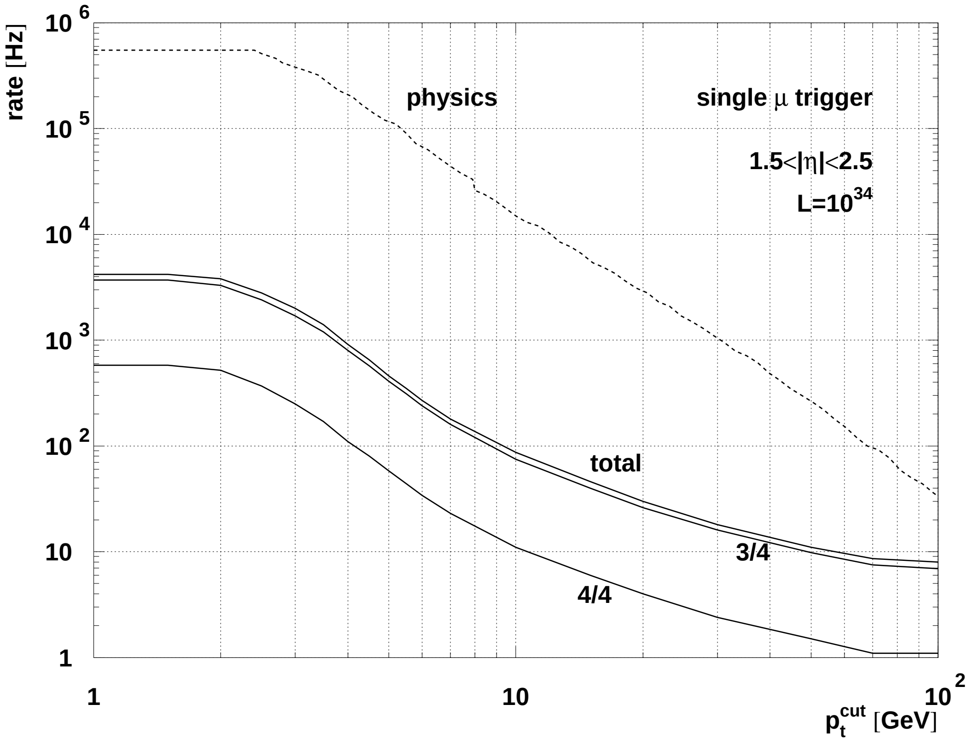

Figure 4: Trigger rate due to n's and γ's from 3-fold and 4-fold coincidencies.

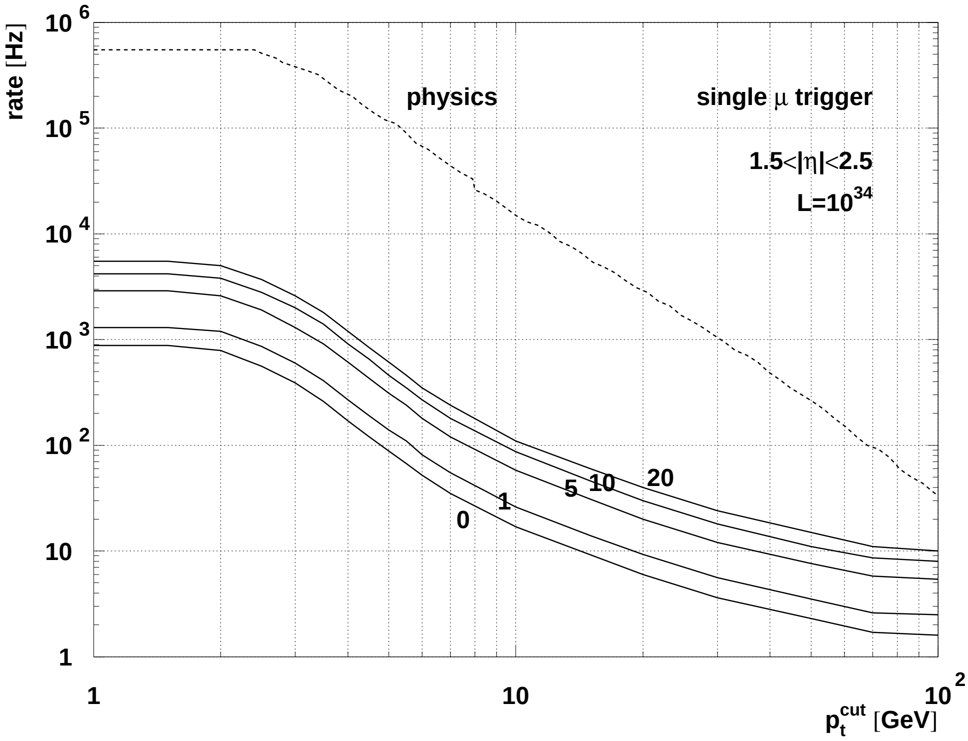

Figure 5: Trigger rate due to n's and γ's for various P^{dead} [%].

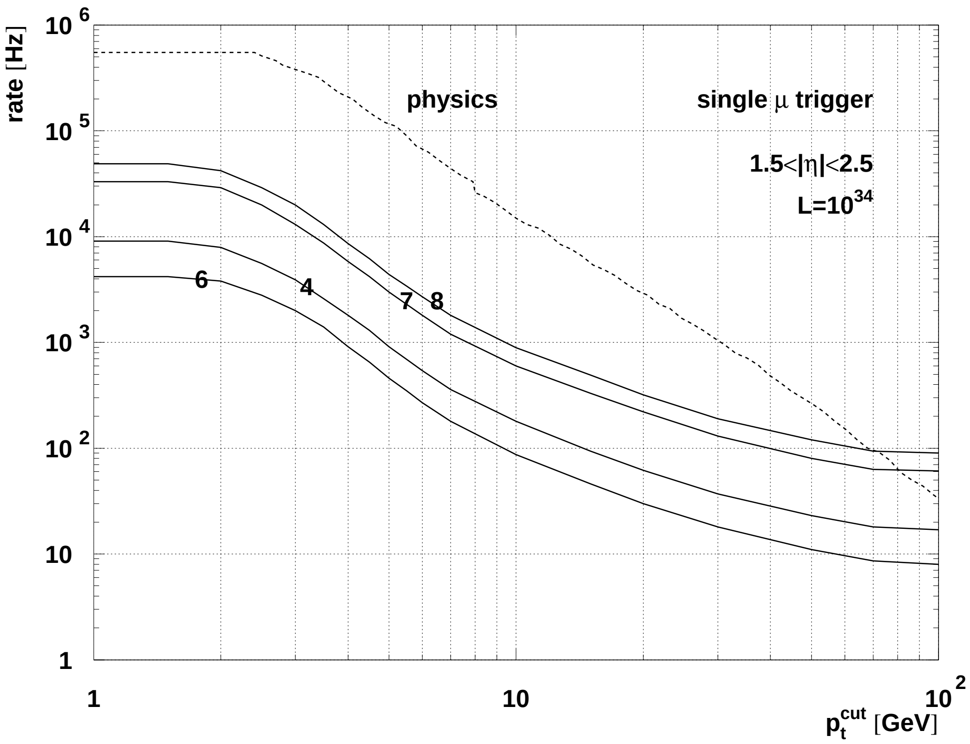

Figure 6: Trigger rate due to n's and γ's for various shielding setups described in [1].

The different shieldings are compared in Fig. 6. The figure confirms the general conclusion of the simulation studies [1] that the proper shielding is a crucial element of dealing with netral particle background.

6 Dependence on the trigger granularity and the time resolution

Since the rate from 3-fold coincidence dominates, it is enough to consider only this case. According to the formula 12 this rate is proportional to $P_{3/4}$ and N_{val}. The 3-fold coincidence probability $P_{3/4}$ is proportional to the third power of the strip size s and of the trigger gate t_{gate}. Hence if the time resolution of the whole system (RPC, cabels and front-end) is better then 25 ns we can reduce t_{gate} and thus lower the accidental rate.

Concerning the dependence on the strip size s we have to consider separately granularity in η and in φ. Changing the first one does not change (in the first approximation) the number of patterns N_{val}. Thus the rate is simply proportional to the third power of the strip lenght.

Dependence of the granularity in φ is more complicated bacause it effects the number of patterns N_{val}. If we assume that all patterns in a certain cone are valid then $N_{val} \propto N^3_{s/s}$ i.e. $N_{val} \propto s^{-3}$. Thus both factors cancel one another and the rate does not depend of the granularity. In other words the trigger is done by the coincidence of some fraction of the sector area, no matter how it is segmented. However the pattern based trigger can be more selective and it can reject e.g. zig-zag like patterns from the cone of interest. In that case N_{val} rizes slower than $N^3_{s/s}$ and the total rate decreases with increasing granularity. More quantitative answer needs detailed simulation of various granularities which is foreseen for the near future.

7 Conclusions

The false trigger rate due to neutral particles is well below the rate of real muons in all the discussed cases. However this rate rizes with the third power of the rate of the background hits (the 3-fold rate dominates over the 4-fold one). Thus, if the particles fluxes and/or RPC efficiencies are underestimated e.g. by factor 5 then the false trigger rate can even exceed the one from real muons. Therefore the problem should be carefully watched during further optimization of the detector. Especially:

- neutral particle fluxes should be reduced as much as possible by proper shielding,
- dead areas should be minimized,
- trigger algorithm should avoid 3-fold coincidences wherever possible,
- the trigger granularity should not be degraded, especially in η,
- the trigger gate should be possibly short.

If the final rate is still to high one can consider limiting η-range of the single muon trigger. Since the rate increases with η, one can decrease it significantly on the expense of a lose in statistics which may be tolerable, especially for very hard processes.

Presented study does not take into account coincidences of background hits with hits caused by real muons. For this a simultaneous simulation of the two sources is needed followed by the detailed simulation of the trigger algorithm. The work on this subject is actually going on.

Also the calculation of fluxes and chamber efficiences are continued. The next iteration will include optimizing the shielding, more detailed geometry of the muon stations and tuning the Monte Carlo to the experimental results.

References

[1] M. Huhtinen, P. A. Aarnio, *Radiation problems at LHC experiments, I: Neutral particle background*, CMS technical note **CMS TN/94-135** and University of Helsinki preprint **HU-SEFT R 1994-01**.

[2] *CMS Status Report and Milestones*, **CERN/LHCC 93-48**.

[3] *CMS Letter of Intent*, **CERN/LHCC 92-3**.

[4] H. Czyrkowski et al., *RPC Based CMS Muon Trigger, Progress Report*, CMS technical note **CMS TN/93-111**.